Monthly Notices of the ROYAL ASTRONOMICAL SOCIETY

MNRAS **461,** 1868–1874 (2016) doi:10.1093/mnras/stw1055
Advance Access publication 2016 May 5

Formation of the G-ring arc

N. C. S. Araujo,[1]★ E. Vieira Neto[1] and D. W. Foryta[2]

[1]*Departamento de Matemática, Univ. Estadual Paulista, 12516-410 Guaratinguetá, São Paulo, Brazil*
[2]*Departamento de Física, Univ. Federal do Paraná, 83531-940 Curitiba, Paraná, Brazil*

Accepted 2016 May 2. Received 2016 May 2; in original form 2014 December 10

ABSTRACT

Since 2004, the images obtained by the *Cassini* spacecraft's on-board cameras have revealed the existence of several small satellites in the Saturn system. Some of these small satellites are embedded in arcs of particles. While these satellites and their arcs are known to be in corotation resonances with Mimas, their origin remains unknown. This work investigates one possible process for capturing bodies into a corotation resonance, which involves increasing the eccentricity of a perturbing body. Therefore, through numerical simulations and analytical studies, we show a scenario in which the excitation of Mimas's eccentricity could capture particles in a corotation resonance. This is a possible explanation for the origin of the arcs.

Key words: planets and satellites: dynamical evolution and stability – planets and satellites: individual: (Mimas, Enceladus) – planets and satellites: rings.

1 INTRODUCTION

Since 2004, the *Cassini* spacecraft has returned to Earth a copious amount of data about the Saturnian system. In particular, its imaging system has revealed the existence of several small satellites. There are papers (Spitale et al. 2006; Cooper et al. 2008; Hedman et al. 2010) showing that Mimas perturbs the orbits of some of these satellites by resonant interactions.

In 2006, data returned by *Cassini* revealed an arc of dust inside the G ring. Since then, this region has been explored by Hedman et al. (2007), who precisely calculated the mean motion of the G arc using *Cassini* data. They revealed that this arc is in a 7:6 corotation resonance with Mimas. Through the analysis of images obtained between 2008 and 2009, it was found that the satellite Aegaeon was located inside this arc (Hedman et al. 2010). Since this satellite is immersed in this arc, it is also trapped in this corotation resonance with Mimas.

Hedman et al. (2010) confirmed this corotation resonance through numerical simulations of the full equations of motion. They also identified that this satellite is in a corotation resonance with characteristic angle:

$$\varphi_{\rm CER} = 7\lambda_{\rm Mimas} - 6\lambda_{\rm Aegaeon} - \varpi_{\rm Mimas}. \quad (1)$$

Their simulations also show that a nearby Lindblad resonance also influences the moon's motion (Hedman et al. 2010).

Prior to this study and also from *Cassini* images, two other satellites were discovered: Methone in 2004 (Spitale et al. 2006) and Anthe in 2007 (Cooper et al. 2008). A numerical analysis of the full equations of motion (Spitale et al. 2006; Cooper et al. 2008) indicates that these satellites are in corotation resonances whose characteristic angles are, respectively,

$$\varphi_{\rm CER} = 15\lambda_{\rm Methone} - 14\lambda_{\rm Mimas} - \varpi_{\rm Mimas}, \quad (2)$$

$$\varphi_{\rm CER} = 11\lambda_{\rm Anthe} - 10\lambda_{\rm Mimas} - \varpi_{\rm Mimas}. \quad (3)$$

The *Cassini* images also show that Aegaeon, Anthe and Methone are immersed in tenuous arcs of particles (Hedman et al. 2007, 2009). Hedman et al. (2010) said that these particles probably originated from the material knocked off, at low speeds, from the surface of these satellites. Therefore, these particles do not have enough energy to escape the corotation resonance and then remain close to the satellite, filling the nearby space. With this evidence, Hedman et al. (2010) concluded that the study of these satellites and their arcs may improve our understanding of the connection between satellites and rings. Because these objects and their arcs are in corotation resonances, these satellites may be seen as a distinct class of objects in the Saturn system.

The existence of these satellites immersed in arcs of dust allows us to infer two possibilities for their origin: (i) The satellites were built up by particles previously caught in resonance and their arcs are the vestiges of this formation. Alternatively, (ii) Mimas captured satellites already formed, and consequently the arcs originated from particles that broke off from these satellites.

Although we are not able to judge immediately which of the above statements is the correct one, we realize that both statements depend on the possibility of bodies being captured in a corotation resonance with Mimas, either small particles or a full satellite. Thus, in this work we investigate the mechanism of capturing particles in a corotation resonance.

A corotation resonance exists only when the perturbing satellite has an eccentricity different from zero (Murray & Dermott 1999). Then, in our problem, corotation depends on the

★E-mail: nilcasr@gmail.com

eccentricity of Mimas. Due to tidal effects, the eccentricity of Mimas should be lower than the current value (Meyer & Wisdom 2008). However, Mimas has a higher eccentricity than most of Saturn's regular satellites. It is likely that its eccentricity increased through a resonant interaction with another satellite. In this work, we will consider that the presence of Enceladus plays an important role in this scenario.

The aim of this paper is to investigate the mechanisms that would make Mimas capture particles in a corotation resonance in the historical Saturn system. The study will be made through numerical simulations and analytical studies, which will be developed using the dynamics of three- and four-body problems considering the effects of the non-spherical shape of Saturn.

In our problem, the main bodies are Saturn, Mimas, Enceladus and the particles of the G ring. We will study the scenario where particles are captured in a corotation resonance with Mimas when Mimas passes through a resonance with Enceladus. As a result of this study, we will have a better understanding of the dynamics involved in the origin and stability of small satellites. In this study, we will focus on a 7:6 corotation resonance.

In Section 2, we briefly discuss corotation resonance. Section 3 introduces the mechanism we develop to obtain the variation of the eccentricity of Mimas. Section 4 shows the effects of this mechanism on Mimas's orbit. Section 5 presents the results of this mechanism when a ring of particles is immersed in the 7:6 corotation resonance region. In Section 6, we analyse the process of capture due to the migration. Finally, the concluding remarks for this study will be found in the Section 7.

2 RESONANCES WITH OBLATE PLANETS

When an object orbits an oblate planet, its orbit experiences the effects of a potential, which depends on the planet's zonal harmonic coefficients: $J_2, J_4, \ldots$. The perturbations of that potential cause the rotation of the orbit in space, or the precession of the unperturbed orbit.

The rotation of the orbit generates three frequencies: n (the mean motion), and κ and ν (the radial and vertical epicyclic frequencies, respectively) (Murray & Dermott 1999). Thereby, considering the additional gravitational effects of a perturbing satellite on a particle, when this system is around an oblate planet, the orbit of the particle can be analysed through those frequencies.

Those frequencies are associated with the precession of the node and pericentre of the orbit by $\kappa = n - \dot{\varpi}$ and $\nu = n - \dot{\Omega}$. From its definition, corotation resonance (Murray & Dermott 1999) occurs when

$$\varphi_{\rm CR} = j\lambda' + (k + p - j)\lambda - k\varpi' - p\Omega', \tag{4}$$

where the primed orbital elements belong to the perturbing satellite while the non-primed orbital elements belong to the particle; j, k and p are integer values.

When a particle is in a corotation resonance with a perturbing satellite, some orbital parameters are modified. There are analytical models able to estimate the extent of these variations, for example, the pendulum model and the Hamiltonian approach (Murray & Dermott 1999). The orbital parameter that is most strongly affected by corotation resonance is the semi-major axis. Using the pendulum model, we can calculate the maximum width libration of the semi-major axis for the corotation resonance.

The maximum width for a corotation resonance is (Murray & Dermott 1999, equation 10.10)

$$W_{\rm CR} = 8\left(\frac{a|R|}{3Gm_{\rm p}}\right)^{1/2} a, \tag{5}$$

where a is the semi-major axis of the perturbed body, $m_{\rm p}$ is the central body's mass and R is the relevant term of the perturbing function, whose equation is

$$R = \frac{Gm'}{a'} f_{\rm d}(\alpha) e'^{|k|} s'^{|p|} \cos\varphi_{\rm CER}, \tag{6}$$

where the primed parameters are for the perturbing satellite, and m', a', e' and s' are the mass, semi-major axis, eccentricity and a value associated with the inclination I', i.e. $s' = \sin(I'/2)$. $f_{\rm d}(\alpha)$ is a function in Laplace's coefficients for the direct terms of the perturbing function, $\varphi_{\rm CER}$ is the corotation resonant angle, and k and p are integers.

Therefore, from the above equations, we expect that for the existence of a corotation resonance, the perturbing satellite's eccentricity must be different from zero.

3 MODEL

The current eccentricity of Mimas is approximately 0.02. Meyer & Wisdom (2008) pointed out that this value is relatively high and would imply a much higher value in the past, or it was recently excited. It is known that the eccentricity of a satellite can be excited due to resonances (Murray & Dermott 1999), but the recent value of Mimas's eccentricity cannot be explained by present resonances such as the Mimas–Tethys 4:2 mean motion resonance (Champenois & Vienne 1999; Callegari & Yokoyama 2010). Thus, we suppose that Mimas experienced some event in the past that increased its eccentricity.

Meyer & Wisdom (2008) suggested that Mimas was captured by Enceladus or by Dione into a resonance when the eccentricity of Mimas was less than the current value. They verified that if Mimas came into some eccentricity-type resonance with one of these satellites, Mimas's eccentricity increased and even exceeded its current value. After these satellites escaped from this resonance interaction, the tidal orbital evolution decreased their eccentricity to the current values, as we can notice in figs 6, 7 and 9 from the paper of Meyer & Wisdom (2008). Therefore, these kinds of resonant encounters could have temporarily increased Mimas's eccentricity, which would have favoured the capture of particles in Mimas's corotation resonances.

In our study, we adopt a scenario where we have a Mimas–Enceladus 3:2 e-Mimas resonance[1] as discussed in Meyer & Wisdom (2008). That resonance would induce an increase in Mimas's eccentricity even larger than the current one, and after a certain time those satellites would go out of that resonance. After the escape, due to tidal effects, the eccentricity of Mimas would decay to the current value (Meyer & Wisdom 2008).

In our scenario, Mimas and Enceladus were closer to Saturn than they are today. Thus, we had to calculate a consistent position for them based on a satellite tidal evolution. For this task, we perform the procedures discussed below.

First, we evaluate the ratio of the semi-major axes α when Mimas and Enceladus were trapped in the 3:2 eccentricity mean motion

[1] e-Mimas resonance is the notation of Meyer & Wisdom (2008) for Mimas's eccentricity-type first-order resonance.

resonance. When two satellites are in mean motion resonance, α remains approximately constant and can be calculated with (Champenois & Vienne 1999)

$$\alpha = \left(\frac{p+q}{p}\right)^{-2/3}\left(1+\frac{q_1\dot{\varpi}_{\rm M}+q_2\dot{\varpi}_{\rm E}+q_3\dot{\Omega}_{\rm M}+q_4\dot{\Omega}_{\rm E}}{n_{\rm E}(p+q)}\right)^{-2/3}, \quad (7)$$

where p, q, q_1, q_2, q_3 and q_4 are integers. $\dot{\varpi}_{\rm M}$, $\dot{\varpi}_{\rm E}$, $\dot{\Omega}_{\rm M}$ and $\dot{\Omega}_{\rm E}$ are the precession rates of the longitude of the pericentre and the longitude of the ascending node for Mimas and Enceladus, respectively, and $n_{\rm E}$ is the mean motion of Enceladus. Using the angles for the 3:2 eccentricity mean motion resonance in equation (7), we get the ratio between the semi-major axes of Mimas and Enceladus when they were trapped in that resonance (Champenois & Vienne 1999). In this paper, the values of $\dot{\varpi}_{\rm M}$, $\dot{\varpi}_{\rm E}$, $\dot{\Omega}_{\rm M}$ and $\dot{\Omega}_{\rm E}$ are consistent with the geometric orbital elements (Renner & Sicardy 2006). For our resonance, we find the values of q_1, q_2, q_3 and q_4 from the comparison with the general resonant angle:

$$\varphi = p\lambda - (p+q)\lambda' + q_1\varpi + q_2\varpi' + q_3\Omega + q_4\Omega', \quad (8)$$

where λ, ϖ and Ω are the mean longitude, the longitude of the pericentre and the longitude of the ascending node for the inner satellite, while those longitudes with a prime represent the angles for the outer satellite, with resonant angle as

$$\varphi_e = 2\lambda_{\rm M} - 3\lambda_{\rm E} + \varpi_{\rm M}, \quad (9)$$

where $\lambda_{\rm M}$ is the mean longitude of Mimas and $\lambda_{\rm E}$ is the mean longitude of Enceladus. After our evaluations, we obtain $\alpha = 0.763\,7895$.

The next step was to find the semi-major axes of the satellites corresponding to our α. We call these ancient semi-major axes and they can be evaluated through (the development of the following equation can be seen in Appendix A):

$$a_{0\rm M} = \left[\frac{a_{\rm M}^{13/2}\left(\frac{m_{\rm E}}{m_{\rm M}}\right) - a_{\rm E}^{13/2}}{\left(\frac{m_{\rm E}}{m_{\rm M}}\right) - \frac{1}{\alpha^{13/2}}}\right]^{2/13}, \quad (10)$$

where $a_{0\rm M}$ is Mimas's ancient semi-major axis. $a_{\rm M}$, $a_{\rm E}$, $m_{\rm M}$ and $m_{\rm E}$ are the current semi-major axes and masses of the satellites Mimas and Enceladus, respectively.

Equation (10) is a function of α, the ratio of Mimas's and Enceladus's semi-major axes. As we used a value of α when both satellites were in resonance with each other, we can locate the ancient semi-major axis of Enceladus using $a_{0\rm E} = a_{0\rm M}/\alpha$. The results for $a_{0_{\rm E}}$ and $a_{0\rm M}$ indicate that those satellites were more distant from each other in the past compared with their current positions. This is expected, since the inner satellite migrates faster than the outer one.

The values of Mimas's and Enceladus's ancient semi-major axes, calculated through equation (10), are approximate. To obtain values that lead the system into resonance, we try values near the ancient semi-major axes until we get close to being on the verge of resonance.

The tidal effect can cause Saturn's satellites to migrate with a velocity of order between 10^{-7} and 10^{-5} km yr^{-1} at their current positions (Meyer & Wisdom 2008; Lainey et al. 2012). Therefore, we should migrate Mimas and Enceladus with velocities close to those velocities. However, doing that would take a long computational time, as we have noted in migration tests using that order of magnitude for the migration rate. As we are trying to prove the concept of corotation eccentricity resonance capture caused by the eccentricity of Mimas when it was larger due to mean motion resonance with Enceladus, we used values that speeded up our simulations. Thus, we migrate Mimas with a rate for the semi-major axis close to 1 km yr^{-1} and Enceladus around 0.01 km yr^{-1}. The external satellite will migrate slower than the internal one (see equation A3 and also Burns & Matthews 1986). To generate those rates, we inserted a drag force into the dynamics for each satellite:

$$\vec{F}_{\rm p} = -\gamma v\vec{v}, \quad (11)$$

where $\vec{v}$ is the velocity of the satellite and γ a constant that will give the mentioned velocities for the semi-major axes. The semi-major axes will increase due to the negative sign of γ.

In a scenario with a lower eccentricity for Enceladus, using the three-body dynamics for Saturn, Mimas and Enceladus, we found no chaotic behaviour for the resonance angle when we have the Mimas–Enceladus 3:2 e-Mimas resonance. That is, we found the same results as Meyer & Wisdom (2008) for the Mimas–Enceladus 3:2 e-Enceladus resonance. This means that Mimas does not escape from the resonance capture during our time integration. This integration was run for 3000 yr of arbitrary time (equivalent approximately to 300 million years, if we had used the correct rates for the migration).

Tidal effects could have reduced the higher eccentricity of Enceladus, and in our scenario we verified that this higher eccentricity is necessary for Mimas to escape from the resonance. Higher values for Enceladus's eccentricity are possible due to earlier captures into other resonances, as can be seen in Meyer & Wisdom (2007).

We used, respectively, 0.005 and 0.02 for the initial eccentricities of Mimas and Enceladus. These values make our scenario work very well, as we will show below. Probably, other mechanisms may exist that could take Mimas out of the resonance other than this value for the eccentricity of Enceladus, but we are most interested in proving that the corotation resonance is able to capture particles, and we will investigate those features in other works.

4 MIGRATION EFFECTS ON MIMAS'S ORBIT

In the first part of our hypotheses, we treat the excitation of Mimas's eccentricity as due to its passage through the Mimas–Enceladus 3:2 e-Mimas resonance during the migration process of these satellites. To perform this simulation, we used the Gauss–Radau spacings described by Everhart (1985) with an initial time step of 0.1 d. The dynamics of this process included Mimas, Enceladus and an oblate Saturn, and also the drag force of equation (11). For the initial conditions of Mimas and Enceladus, we use the considerations noted in Section 3 to form the set of initial conditions shown in Table 1.

In Fig. 1, we observe the behaviour of the critical angle for the Mimas–Enceladus 3:2 e-Mimas resonance (equation 9). This behaviour occurs due to the passage of Mimas and Enceladus through the resonance during the migration process. We can see that at the very beginning of the simulation, the Mimas–Enceladus system was not in resonance (the resonant angle circulates) and, due to the system migration, those satellites enter the Mimas–Enceladus 3:2 e-Mimas resonance (Meyer & Wisdom 2008) in which the resonant angle librates around 0°. We can see that during the migration process there is a decreasing amplitude for the resonant angle, which may make the resonance between them more robust. Subsequently, this amplitude begins to increase until it reaches 180°. At this point, we can say that Mimas and Enceladus are out of resonance.

In Fig. 2(a), we can see the behaviour of Mimas's and Enceladus's semi-major axes during the migration process. Before they enter into resonance, the variation rates for the semi-major axes are the ones stated in the last section, with Enceladus migrating slower than Mimas (see the inset of Fig. 2a). After they enter into resonance, the rate of variation of Enceladus's semi-major axis increases until it reaches a value slightly larger than that of Mimas, while the rate

Table 1. Initial conditions for orbital elements of Enceladus and Mimas, after changes noted in Section 3.

Parameter	Value
Mimas	
Mass	3.75×10^{22} g
Radius	198.8 km
a	$1.799\,177 \times 10^{5}$ km
e	5.0×10^{-3}
I	1.563 223 deg
Ω	$3.564\,454 \times 10^{2}$ deg
ϖ	$1.899\,002 \times 10^{2}$ deg
λ	$3.166\,168 \times 10^{2}$ deg
Enceladus	
Mass	10.805×10^{22} g
Radius	252.3 km
a	$2.354\,949 \times 10^{5}$ km
e	2.0×10^{-2}
I	$5.067\,876 \times 10^{-3}$ deg
Ω	$2.633\,612 \times 10^{2}$ deg
ϖ	$2.822\,281 \times 10^{2}$ deg
λ	$2.950\,096 \times 10^{2}$ deg

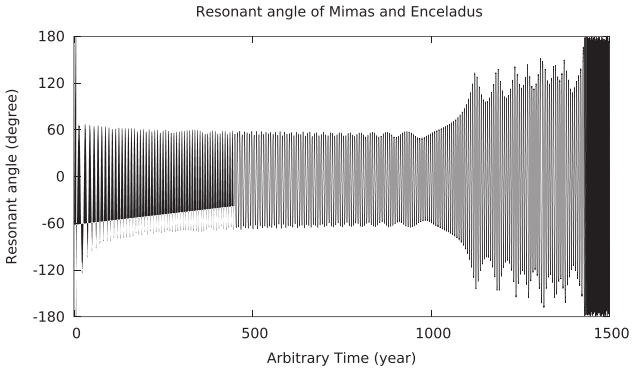

Figure 1. Critical angle for the Mimas–Enceladus 3:2 e-Mimas resonance (equation 9) during the migration process, showing libration around zero. To the end of the tandem migration, the critical angle increases its sweep following the increase of the eccentricity of Mimas.

of variation of Mimas's semi-major axis decreases, which can be seen in the inclination of the semi-major axis in Fig. 2(a). When they come out of resonance, the variation rates for the semi-major axes return to their previous values.

This passage through the resonance affects Mimas's eccentricity significantly, as shown in Fig. 2(b). When Mimas is in resonance, its eccentricity increases to high values while Enceladus's eccentricity remains constant. Despite the migration velocity we have adopted, the behaviour of Mimas's eccentricity is in agreement with the results of Meyer & Wisdom (2008). The eccentricity only stops growing when it reaches an equilibrium eccentricity (here the value is higher, 0.052, which was also found by Meyer & Wisdom 2008) and the satellites escape from the Mimas–Enceladus 3:2 e-Mimas resonance. Although we do not show this in this work, the eccentricities of Mimas and Enceladus should decrease after they go out of the resonance due to the tidal effects and will reach the current values.

These results show that Mimas's eccentricity could be enlarged and hence affect the width of the corotation resonance. In the next section, we will study this effect on the capture of particles by the corotation resonance.

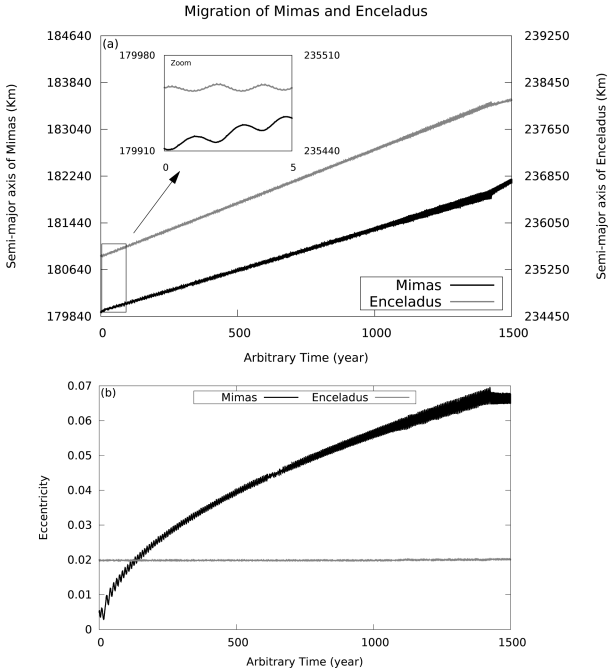

Figure 2. When Mimas is caught in a resonance with Enceladus, its eccentricity grows, as seen in the lower panel. During this time, a tandem migration is established, resulting in a net migration rate that differs from the tidal evolution alone, as seen in the upper plot. The net migration rate of Enceladus increases through the interaction with Mimas, while Mimas's migration rate decreases. This effect ends after the escape from the resonance and the migration rates change, as can be seen at the end of (a).

5 CAPTURE INTO COROTATION RESONANCE

In the previous section, we saw that the eccentricity of Mimas increases when Mimas and Enceladus pass through a 3:2 resonance during the tidal migration process. In this section, we will check if this increase in eccentricity will enable Mimas to capture particles in a corotation resonance. For this study, we created a ring with 10 000 particles in a region where the resonance should appear when the eccentricity of Mimas increases, as we can see in Fig. 3(a). The particles were uniformly distributed with semi-major axes between 162 409.9 and 162 604.8 km and with mean longitudes between 0° and 360°. All particles have their other orbital elements fixed: 0.010 758 38 for the eccentricity, 0.004 053 321° for the inclination, 342.0739° for the ascending node and 326.3412° for the longitude of the pericentre. These fixed orbital elements were based on the orbital elements of Aegaeon after it migrated towards Saturn and when it was close to where the resonance should appear. This choice was made to improve our chances of capture. We are not interested in finding the best orbital configuration for the capture, but in the migration process as the cause of the capture into a corotation resonance.

For this experiment, we integrate the full equations of motion for the four-body model (Saturn, Mimas, Enceladus and a particle) plus equation (11) for only Mimas and Enceladus, which represents the tidal interaction of these bodies. We argue that the homogeneous rings do not raise tidal bulges in the planet like moons do, since the particles of rings have no enough mass to tidal effects arise. Also, the ring's particles do not interact with each other by collisions or gravity. We also considered an oblate Saturn for all particles involved in the integration. The integrations were made using the Gauss–Radau spacings described by Everhart (1985) with an initial

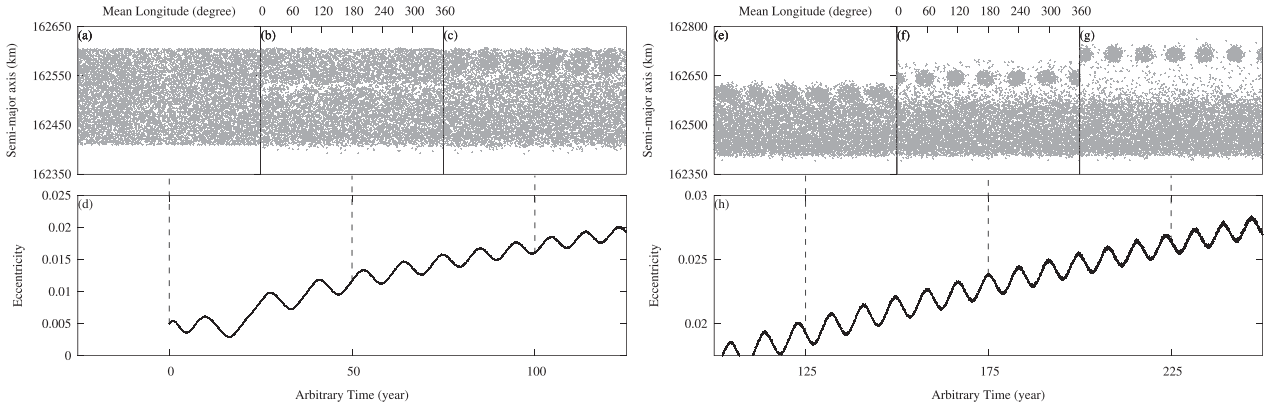

Figure 3. These six snapshots show the evolution of the capture into a corotation resonance. The simulation began with the coupling migration between Mimas and Enceladus. A full ring of particles representing possible bodies that may be captured inside the corotation resonance is shown in grey. In the last snapshot, we can see all the corotation sites that have captured particles and have been conveyed out of the ring by the interaction with Mimas in its migration process.

time step of 0.1 d. We used the same initial conditions for Mimas and Enceladus of Table 1. It is important to say that, although all 10 000 particles were integrated at the same time, they do not interact with each other. Thus, this is a four-body problem including the oblateness of Saturn for each particle.

In the lower panels of Fig. 3, we can see the evolution of Mimas's eccentricity, and in the upper panels, the effects this evolution had on the particles of the ring.

At the very beginning, despite some small variation, Mimas's eccentricity does not increase, as we can see in Fig. 3(d). After some time, the satellites enter the 3:2 e-Mimas resonance and Mimas's eccentricity increases, which affects the ring, as shown in Fig. 3(b).

In Fig. 3(c), it is possible to see particles trapped in the resonance, which have moved upwards due to Mimas's migration. In panels (e), (f) and (g) of Fig. 3, we see this phenomenon more explicitly. We can clearly see six structures moving outside our initial ring. Those six lobes are consistent with a 7:6 corotation resonance. It is also possible to see that some particles were dragged outwards.

To show explicitly that the variation of eccentricity is responsible for the capture into a corotation resonance, we ran another experiment passing the corotation resonance through the ring of particles, but without varying the eccentricity of Mimas. Thus, we take Enceladus out of the simulation and initiated Mimas with its present eccentricity of 0.02 and its semi-major axis of 100 km, below the value shown in Table 1. For all the other orbital elements, we used the values in Table 1, and then applied the migration process to Mimas. The ring of particles was the same as the last experiment.

We noted that the capture of particles does not occur due to overlap between the Lindblad and corotation resonances. These two resonances have a separation of about 19 km (Fig. 4b) and the particles in the ring trapped by the corotation resonance feel the Lindblad perturbation (El Moutamid, Sicardy & Renner 2014). These simulations show that, in our accelerated tidal scenario, the overlap of resonances is not the dominant mechanism in the capture of particles.

We can see that holes appear while the corotation resonance passes through the ring of particles (see Figs 5a–f). As there are no particles inside these holes, we can affirm that particles were not captured. This effect shows that the corotation resonance can neither capture nor lose particles unless it changes its width. However, we can see that some particles stay close to the corotation edge (Figs 5e and 5f). These particles are temporarily captured in a phenomenon known as resonance stickiness (Contopoulos & Harsoula 2010).

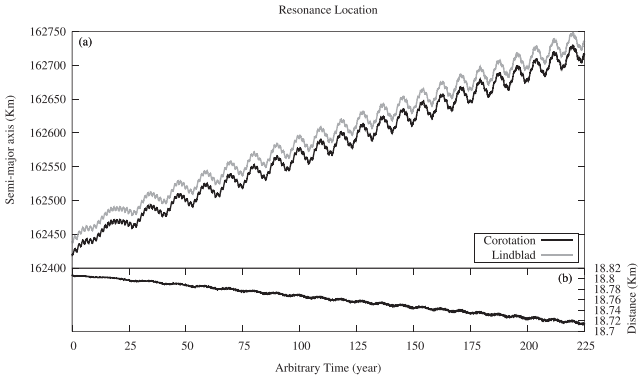

Figure 4. (a) Localization of corotation and Lindlblad resonances. These locations were found following the technique of Foryta & Sicardy (1996), with the equations of Renner & Sicardy (2006). The corotation and Lindlblad locations move because Mimas is migrating during this simulation. (b) Distance between these resonances.

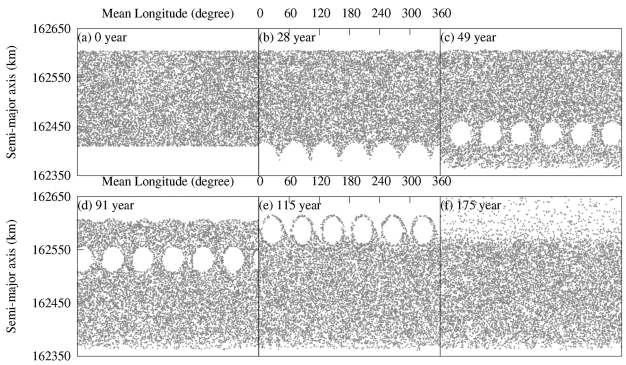

Figure 5. For these six snapshots, we have taken Enceladus out of the simulation. Without the eccentricity enhancement due to the 3:2 resonance, there are no captures into the corotation resonance. In the last snapshot, all corotation sites have passed through the ring without any particle being captured.

These particles move in the border of the lobes of the corotation resonance for a time and then they escape.

With these results, we show that our scenario could explain the formation of the arc of the G ring. In this scenario, we used a migration rate much above that generated by the tidal effect, and with

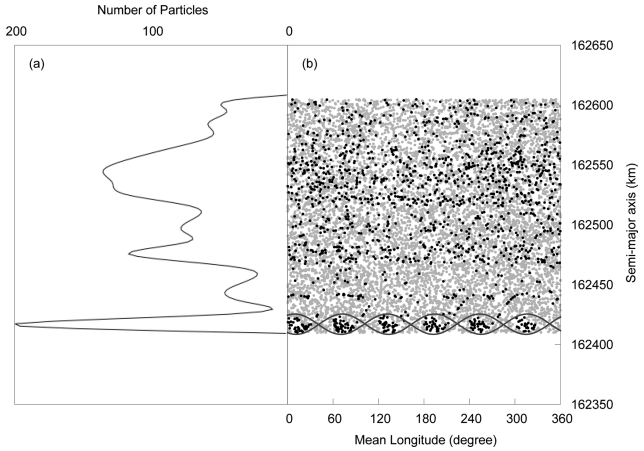

Figure 6. Evolution of the capture into corotation resonance through the ring of particles. (a) Histogram of captured particles in ranges of 10 km for the semi-major axis. (b) Initial conditions of the captured particles.

a realistic migration rate, it must work in the same way. Actually, we did our first experiments with rates consistent with the tidal migration and observed the robustness of the corotation resonance.

In one of our first experiments, which we have not shown here, we created an arc of 1847 particles in the resonance of Mimas where the G-ring arc was on 2004 January 1 (Hedman et al. 2010), and simulated Mimas migrating with a velocity equal to 9.0×10^{-9} km yr^{-1} towards Saturn for 1000 yr. From the simulation, we found that 98 per cent of the particles were in corotation with Mimas, corroborating the robustness of the corotation resonance.

In this scenario, a high initial eccentricity was needed for Enceladus to force the escape of Mimas from the 3:2 e-Mimas resonance, but it is not a problem for our scenario because several other processes could take Mimas out of this resonance, for instance, an eventual resonance between Mimas and Dione.

6 EVOLUTION OF THE CAPTURE RESONANCE

In the last section, we observed that the particles were captured in a corotation resonance and were dragged out of the ring we created. Now we will analyse the history of the captures. In Fig. 6, we have a ring of particles at time 0 of our simulation and we indicate the particles that were captured. In Fig. 6(b), we have identified with grey points the particles that were not captured in the Mimas migration process and with black points the particles that were captured in this process and did not escape the corotation sites during the simulation. The final state of these captured particles (black points in Fig. 6b) can be seen in Fig. 3(g) occupying the corotation sites above the ring of particles.

In the bottom part of Fig. 6(b), we see a draft of the 7:6 corotation sites in the initial condition produced by Mimas's eccentricity. The amplitude of the curves obeys the width of the corotation for the initial Mimas eccentricity (equation 5). With Mimas's migration, the width of this curve will enlarge. This enlargement will produce the captures in the corotation resonances.

We can see in Fig. 6(b) that the black points are spread in the ring and they show some structures. In panel (a), we show the number of captured particles in bins of 10 km for the semi-major axis. The excess of particles in the low part of the disc occurs due to Mimas's initial eccentricity, as the corotation resonance has an initial width that is shown by the embedded black points encircled by the draft

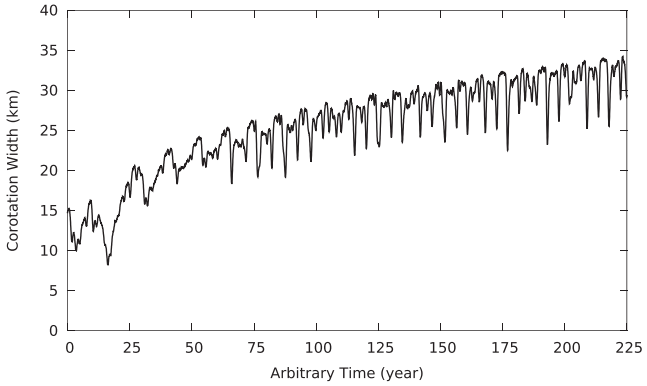

Figure 7. Amplitude evolution of the corotation resonance width based on equation (5) for each value of Mimas's eccentricity of Fig. 3.

representing the corotation curves. The structures and the histogram suggest that we do not have a homogeneous rate of captures. Thus, capturing is not continuous, but occurs in steps. This is explained since the eccentricity oscillates while it increases, as shown in the graphs of Fig. 3.

The capture by the corotation resonance is complex. When Mimas was captured by the 3:2 resonance with Enceladus, its eccentricity began to increase but not in a uniform way. In Fig. 7, we see the evolution of this width based on equation (5) and the history of Mimas's eccentricity shown in Fig. 3. The net result of the process doubles the initial width; however, locally it increases and decreases in a very noisy form. Thus, some particles were captured while others escape from the corotation resonance. The particles that were captured and escaped are the ones in the stickiness caused by the corotation resonance observed in Fig. 5. This complex dynamic explains the structures observed in Fig. 6.

This feature can be understood when we consider the capture probability in the corotation resonance, which depends on perturbing the eccentricity (Quillen 2006). In our case, the perturber is Mimas. Mimas's eccentricity increases non-uniformly (Fig. 3), so the capture probability oscillates during the simulation. An increase of eccentricity favours the capture, and when it decreases, the likelihood of escape increases. The result is a relative capture probability, because sometimes particles are more likely to be captured, but sometimes less likely. This creates the structures observed in Fig. 6.

These results lead us to conclude that the migration sweeping over the particles, as shown in Fig. 3, with the change in the corotation resonance width producing a change in Mimas's eccentricity, as shown in Fig. 6, is the process that could explain the capture of the one particle, or a group of particles, that produced the arc of the G ring.

7 CONCLUSIONS

In this paper, we showed that it is possible to explain the formation of the arc of the G ring through a plausible scenario where Saturn's tides play the main role.

Saturn's tides could vary the semi-major axis of the satellites, which make them cross several resonances. In this process, Mimas's low eccentricity could have increased and could have caused the enlargement of the corotation region.

In our experiment, when Mimas created the region of corotation particles, all six structures of the corotation were populated. Thus, if there were a ring of particles in the corotation resonance capture region, we should observe other groups today. However, there exists

only one arc. Our hypothesis is still plausible, since other effects, such as Poynting–Robertson drag, may have destroyed the other groups, or even the region was not as homogeneous as we created them in this scenario. We believe that further studies on the formation of the G-ring arc may solve this problem. Other studies could also answer if the arc was formed by agglomeration or erosion, and all this information could clarify how and why only one group is observed in the 7:6 corotation resonance.

ACKNOWLEDGEMENTS

The authors want to thank Bruno Sicardy for the prolific discussions and helpful suggestions, the anonymous referee for his helpful suggestions, and the Brazilian science funding agencies CAPES, CNPq and FAPESP (grant 2011/08171-3).

REFERENCES

Burns J. A., Matthews M. S., eds, 1986, Satellites. Univ. Arizona Press, Tucson, AZ
Callegari N., Yokoyama T., 2010, Planet. Space. Sci., 58, 1906
Champenois S., Vienne A., 1999, Celest. Mech. Dynamical Astron., 74, 111
Contopoulos G., Harsoula M., 2010, Celest. Mech. Dynamical Astron., 107, 77
Cooper N. J., Murray C. D., Evans M. W., Beurle K., Jacobson R. A., Porco C. C., 2008, Icarus, 195, 765
El Moutamid M., Sicardy B., Renner S., 2014, Celest. Mech. Dynamical Astron., 118, 235
Everhart E., 1985, in Carusi A., Valsecchi G. B., eds, Proc. IAU Colloq. 83, Dynamics of Comets: Their Origin and Evolution, Astrophysics and Space Science Library. Kluwer, Dordrecht, p. 185
Foryta D. W., Sicardy B., 1996, Icarus, 123, 129
Hedman M. M. et al., 2007, Science, 317, 653
Hedman M. M., Murray C. D., Cooper N. J., Tiscareno M. S., Beurle K., Evans M. W., Burns J. A., 2009, Icarus, 199, 378
Hedman M. M., Cooper N. J., Murray C. D., Beurle K., Evans M. W., Tiscareno M. S., Burns J. A., 2010, Icarus, 207, 433
Lainey V. et al., 2012, ApJ, 752, 14
Meyer J., Wisdom J., 2007, Icarus, 188, 535
Meyer J., Wisdom J., 2008, Icarus, 193, 213
Murray C. D., Dermott S. F., 1999, Solar System Dynamics. Cambridge Univ. Press, Cambridge
Poulet F., Sicardy B., 2001, MNRAS, 322, 343
Quillen A. C., 2006, MNRAS, 365, 1367
Renner S., Sicardy B., 2006, Celest. Mech. Dynamical Astron., 94, 237
Spitale J. N., Jacobson R. A., Porco C. C., Owen W. M., Jr, 2006, AJ, 132, 692

APPENDIX A

Poulet & Sicardy (2001) affirm that the attraction of the tidal bulge raised on a planet by a satellite outside the synchronous orbit results in a gain of angular momentum by the satellite. This causes the orbit of the satellite to expand and the rate of change of its semi-major axis is

$$\frac{\dot{a}}{a} = 3\left(\frac{G}{M_\mathrm{p}}\right)^{1/2} k_{2\mathrm{p}} \frac{R_\mathrm{p}^5}{Q_\mathrm{P}} \frac{m}{a^{13/2}}, \tag{A1}$$

where the parameters a, $\dot{a}$ and m are the semi-major axis, its variation and the mass of the satellite. G is the gravitational constant, M_p is the mass of the planet, $k_{2\mathrm{p}}$ is the Love number of the planet and Q_p is the dissipation factor.

We consider that the semi-major axes of Mimas and Enceladus suffered changes described by equation (A1). If we integrate this equation, keeping M_p, $k_{2\mathrm{p}}$ and Q_p constant over time and using the parameters of Mimas and Enceladus, we can find the values of the semi-major axis for Mimas that enables it to become trapped into a resonance with Enceladus in the remote past.

The first consideration is that the physical properties of the planet are constant, so we can write that

$$\xi = 3\left(\frac{G}{M_\mathrm{p}}\right)^{1/2} k_{2\mathrm{p}} \frac{R_\mathrm{p}^5}{Q_\mathrm{P}}, \tag{A2}$$

where ξ is a constant depending on the planet's parameters. Consequently, equation (A1) becomes

$$\dot{a} = a^{-11/2}\xi m. \tag{A3}$$

Integrating it, we have

$$\frac{2}{13}\left(a^{13/2} - {a_0}^{13/2}\right) = \Delta t \xi m, \tag{A4}$$

where the integral constant a_0 is the semi-major axis at t_0, and $\Delta t = t - t_0$. Calculating the value of this integral with the parameters of Mimas, we have

$$\frac{2}{13}\left(a_\mathrm{M}^{13/2} - a_{0\mathrm{M}}^{13/2}\right) = \Delta t_\mathrm{M} \xi m_\mathrm{M}, \tag{A5}$$

where a_M and $a_{0\mathrm{M}}$ are the current and ancient semi-major axes of Mimas, respectively, m_M is Mimas's mass and Δt_M is the time taken for Mimas to vary its position from $a_{0\mathrm{M}}$ to a_M.

Using that integral with the parameters of Enceladus, we get

$$\frac{2}{13}\left(a_\mathrm{E}^{13/2} - a_{0\mathrm{E}}^{13/2}\right) = \Delta t_\mathrm{E} \xi m_\mathrm{E}, \tag{A6}$$

where M was replaced with E.

Now, if we consider that t is the current time and t_0 is an instant when these satellites would be in resonance, we have $\Delta t_\mathrm{M} = \Delta t_\mathrm{E}$. Also, the semi-major axis ratio for Mimas and Enceladus for the resonance is $\alpha = a_{0\mathrm{M}}/a_{0\mathrm{E}}$. Then, from equations (A5) and (A6), we find that

$$a_{0\mathrm{M}} = \left[\frac{\left(\frac{m_\mathrm{E}}{m_\mathrm{M}}\right) a_\mathrm{M}^{13/2} - a_\mathrm{E}^{13/2}}{\left(\frac{m_\mathrm{E}}{m_\mathrm{M}}\right) - \frac{1}{\alpha^{13/2}}}\right]^{2/13}. \tag{A7}$$

Therefore, we calculate with equation (A7) an approximate value for the ancient semi-major axis of Mimas, when that satellite was trapped in resonance with Enceladus, given an appropriate α.

This paper has been typeset from a TEX/LATEX file prepared by the author.